




Unbalanced core detector (UCD): a novel direct-reading dosimeter for FLASH radiotherapy

R. Bedogni¹, L. Russo¹, A. Calamida¹, A. I. Castro-Campoy¹, A. Fontanilla¹, D. Dashdondog¹, M. A. Caballero-Pacheco¹, T. Napolitano¹, C. Cantone¹, A. Pietropaolo^{1,2,a} , G. Felici³

¹ INFN, Laboratori Nazionali di Frascati, via Enrico Fermi 40, 00044 Frascati, Italy

² ENEA Nuclear Department, via Enrico Fermi 45, 00044 Frascati, Italy

³ SIT Sordina IORT Technologies S.P.A., Via dell'Industria 1/A, Aprilia 04011, LT, Italy

Received: 20 December 2023 / Accepted: 10 June 2024

© The Author(s) 2024

Abstract FLASH radiotherapy (FRT) is a novel radiotherapy technique based on dose rates that are several orders of magnitude greater than those used in conventional radiotherapy (40 Gy/s vs. 0.5–5 Gy/min). FRT is still in its preclinical and early clinical stage of development. However these studies indicate that FRT is more effective in sparing normal tissues from radiation-related side effects, as compared to conventional radiotherapy. This is the so-called "FLASH effect" and was observed with multi-MeV electron beams. Before FRT is made available to humans, more basic research is needed to fully understand its radiobiology fundamentals. Meanwhile, suitable radiation sources and dosimetric tools are gradually becoming available. Within this framework, INFN-LNF developed the Unbalanced Core Detector (UCD), a novel type of electron dosimeter designed to operate in the FRT domain. UCD main characteristics are the nearly isotropic response, the independence from the electron energy, the very high radiation resistance, the linearity up to dose rates of MGy/s and the possibility to record the time evolution of a single radiation pulse. UCD was tested using 7 and 9 MeV electron beams produced with the ElectronFlash accelerator from Sordina IORT Technologies (SIT S.p.A.) in Aprilia, Italy. UCD was used to measure dose distributions in a water phantom. The results well compare to those obtained with a flashDiamond detector from PTW.

1 Introduction

Although ultra-high dose rate (UHDR) fields were already used in the 1970s for in vitro radio-oncology experiments [1–4], it was only in 2014 that what is presently known as "FLASH effect" was demonstrated: as compared to a traditional fractionated radiotherapy, an UHDR radiotherapy treatment with the same tumour control probability can produce less severe normal tissue complications [5]. This triggered intense research efforts producing hundreds related papers [6–13], leading to first trials on humans in 2019 [14] and to first follow-up studies, showing no evidence of delayed effects [15]. To date, the FLASH effect was observed not only with multi-MeV electron beams, but also with gammas [16], protons [17] and ions [18].

The radiobiology of the FLASH effect is not fully understood [19, 20], thus more research is needed before the FRT can be made available to humans. Meanwhile, suitable radiation sources and dosimetric tools are gradually becoming available. Novel electron accelerators with UHDR capabilities are already on the market, such as Oriatron eRT6 [21], Mobetron [22] and ElectronFlash [23, 24]. These machines can deliver radiation pulses with duration 1–10 μ s, repetition rate up to hundreds Hz and dose per pulse up to tens of Gy. The instantaneous dose rate may reach MGy/s. Performing accurate dosimetry in UHDR is highly challenging, as conventional radiotherapy dosimeters such as ionization chambers, semiconductors and scintillators tend to lose their linearity at these dose rates [23]. Although passive dosimeters such as radiochromic films and alanine were successfully used [25, 26], efforts to develop suitable active dosimeters are highly needed for the rapid, accurate and effective dosimetry of FRT [27]. Results were obtained by adapting conventional dosimeters to UHDR, as illustrated below:

- In ionisation chambers, the main disrupting effect of UHDR is the charge loss by recombination. This was limited by using a free-in-air parallel plate chamber with 0.25 mm electrode distance [28]. Such a device can linearly operate up to few Gy/pulse with 9 MeV electrons. Another solution was hypothesised by using a noble gas at appropriate pressure [29].
- Specifically designed, radiation hard, semiconductors were used in UHDR, such as the flashDiamond Detector T60025, available for research purposes from PTW [30]. This was proved to linearly operate up to 20 Gy/pulse with 9 MeV electrons. Silicon Carbides are also under investigation and their operation is currently limited to about 2 Gy/pulse [31].

^a e-mail: antonino.pietropaolo@enea.it (corresponding author)

All mentioned devices operate in time-integrated mode, providing the delivered dose at the end of an exposure without providing the time structure of a single radiation pulse.

A different approach was followed at INFN-LNF with UCD (Unbalanced Core Detector). UCD is an electric sensor whose pins are isolated in absence of radiation. The exposure to intense radiation field causes an electric current that is measured with an especially designed variable-gain front-end electronics. Due to pending initiatives to protect IP, no internal details of UCD are disclosed here. However, the following Sections full describe the results of the characterisation tests. These were performed using ElectronFlash electron machines at SIT Sordina IORT Technologies S.P.A. (Aprilia, Italy), hereafter called SIT. Importantly, UCD can provide time-resolved information on the UHDR pulse, thus allowing to: (1) check the pulse-to-pulse reproducibility in an irradiation session, and (2) detect pulse delivery errors and machine instabilities. These properties are especially important in view of the clinical transition of FRT.

2 Materials and methods

The Unbalanced Core Detector (UCD) (Fig. 1) is formed by:

- A 6 mm diameter spherical sensitive nucleus (patent in progress). In principle, the nucleus can be manufactured virtually in any geometry and size, the spherical geometry being the most suited for clinical dosimetry because of its intrinsic isotropic response. According to experimental tests performed at SIT, the dosimeter sensitivity roughly linearly increases with the radius of the nucleus. Another aspect is the manufacturing process: to date the UCD is manually cabled, so nucleus sizes in the order of few mm are better handled. On the other hand the nucleus should be as small as practically achievable, in order to minimally perturb the radiation field. 6 mm diameter is the result of an optimisation process involving these three aspects. Due to its size, the UCD is characterised by an inherent "build up" layer estimated in 4 mm of water equivalent. The effective measurement point coincides with the geometric centre of the spherical nucleus.
- A water-proof 3D-printed cap with 41 mm height, 8.2 mm inner diameter and 0.5 mm thickness.
- A one-meter long coaxial cable connecting the UCD to the front-end electronics through an SMA straight male connector.

The front-end electronics is based on an ultra-low background, double stage, buffered amplifier with adjustable gain. Importantly, the gain is adjusted from the control PC in order to minimise the number of times the user needs to accede the irradiation room. The analogue board output is sent to a commercial digitizer located in the control room. The cable connecting the board to the digitizer can be as long as about 100 m. From the circuitual point of view, UCD can be schematized as a current generator, where the current is proportional to the incident dose rate. The front-end converts this current into a voltage drop. Therefore the time-integrated voltage, usually measured in $V \times \mu s$, is assumed to be proportional to the dose.

The characterization of UCD was performed using an ElectronFlash LINAC (<https://www.soiort.com/flash-rt-technology>) with the following operation parameters:

- Horizontal beam;
- Electron energy 7 and 9 MeV;
- Pulse duration 5 μs and repetition rate 5 Hz;
- An IORT-type PMMA cylindrical applicator with 100 mm diameter was used to homogenise the spatial distribution of the beam;

Fig. 1 The unbalanced core detector

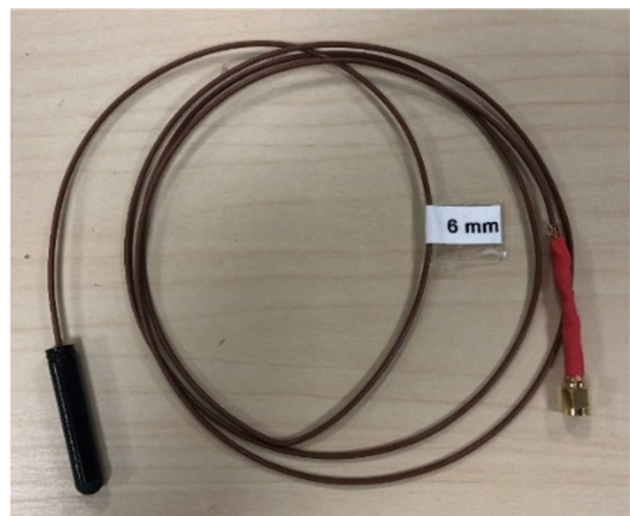


Fig. 2 UCD installed in the water phantom

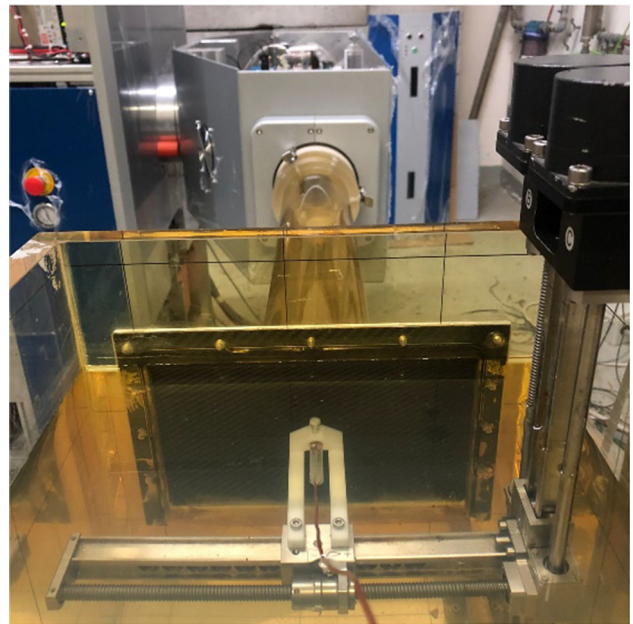
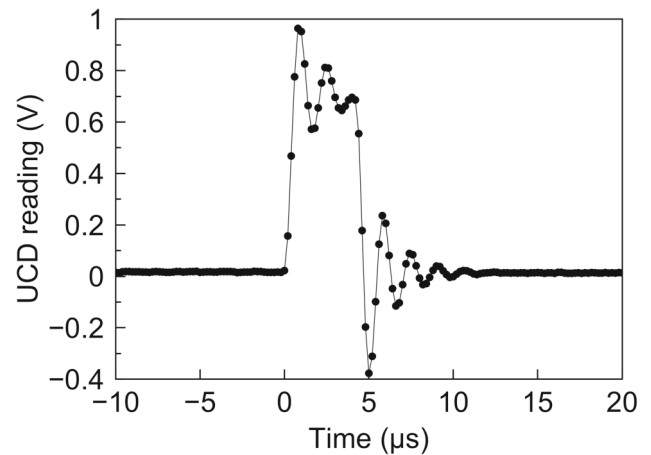


Fig. 3 A typical electron pulse as acquired by a 5 MS/s digitiser connected to the output of the analogue board



- The detector was exposed in a 29.5 cm × 29.5 cm × 40 cm water phantom through a holder which can be remotely moved along the three axes (See Fig. 2). The water phantom has 2 cm thick PMMA walls excepted in the beam entrance area, where the wall is minimised through a carbon fiber. By multiplying this number by the quotient of the electron stopping power in carbon and water, it can be obtained that the corresponding thickness of water is 1.3 mm.
- Each measurement in the water phantom was obtained by delivering 30 pulses.

Figure 3 presents a typical electron pulse as acquired by a 5 MS/s digitiser connected to the output of the analogue board. The oscillations are due to the large intrinsic capacity of the detector. As they have null integral, they do not impact the measurement linearity. Nevertheless, efforts are in progress to compensate them with an adequate filter on the analogue board.

All measurements were simultaneously taken with UCD and a PTW flash Diamond detector T60025 [15].

The following measurements were performed:

1. Percentage Depth Dose (PDD) curves;
2. Lateral beam profiles;
3. Calibration;
4. Linearity;
5. Isotropy;
6. Radiation resistance.

3 Results

Figures 4 and 5 report the percentage depth dose (PDD) curves for 7 and 9 MeV electron beams recorded with both UCD (diameter 6 mm) and the flashDiamond. For both dosimeters the measurement reproducibility was better than 1%, and the main source of uncertainty was the positioning. The positioning uncertainty was transferred to the dose profile by applying Eq. (1), where the positioning uncertainty was assumed to be $\Delta x = 1$ mm. Both UCD and flashDiamond profiles are affected by the same uncertainties ranging from less than 1%, below 20 mm, to about 10% in the falling edge after the maximum.

$$\Delta D = \frac{dD}{dx} \times \Delta x \quad (1)$$

It should be noted that the smallest measured depth for the flashDiamond is about 4 mm lower than UCD. This is due to the UCD physical size, causing an intrinsic build-up of about 4 mm, as mentioned in Sect. 3. Apart this effect, the PDDs of UCD and flashDiamond are indistinguishable.

The lateral beam profiles obtained with both UCD (6 mm diameter) and the flashDiamond at 7 MeV (depth in water 12.5 mm) and 9 MeV (depth in water 17.5 mm) are reported in Figs. 6 and 7. Again, the uncertainty bars are obtained according to Eq. (1) and are associated to UCD for a better inspection of the graphs. The structure of the profile, clearly reflecting the shape of the 100 mm diameter PMMA applicator, is equally described by both dosimeters.

The sensitivity of UCD (6 mm diameter) was estimated by comparison with the flashDiamond at 7 and 9 MeV. The devices were exposed at the same time in five positions within the water phantom. As this procedure can be affected by mutual perturbation effects, it cannot be regarded as a true calibration. However, it has the advantage of using the same beam at the same time. By averaging the FlashDiamond / UCD ratio (q) over the five measurement position, the following values were obtained:

$$q_{av}(7 \text{ MeV}) = (1.17 \pm 0.03) \text{ Gy} \times V^{-1} \times \mu s^{-1}$$

$$q_{av}(9 \text{ MeV}) = (1.19 \pm 0.02) \text{ Gy} \times V^{-1} \times \mu s^{-1}$$

As is known that the energy dependence of flashDiamond is limited to $\pm 1\%$ over the clinical electron beam qualities from 6 to 18 MeV [32], it can be claimed that UCD has similar energy dependence for 7 and 9 MeV beams.

UCD linearity was verified by exposing it in air, covered by a 15 mm thick build-up cap, at different positions in front of the 9 MeV beams. The positions were previously characterised using a combination of radio-chromic films and the toroidal coil-based monitor system of the ElectronFlash machine. As shown in Fig. 8, UCD behaves linearly up to a delivered dose per pulse of about 25 Gy at least. As the pulse duration was 4 μs , this corresponds to about 6 MGy s^{-1} .

Preliminary assessment of the UCD (6 mm diameter) angular response was done by exposing the detector in air, as schematised in Fig. 9. As shown in Fig. 10, the response loss due to the incidence angle is only 7% when the incidence angle varies from 0° to 60° . To thoroughly assess this characteristic, an experiment in water is planned for the near future.

UCD radiation hardness was studied at 9 MeV in air by exposing the device in a fixed position and by gradually increasing the accumulated absorbed dose up to 200 kGy. The delivered dose was estimated using a combination of radio-chromic films and the toroidal coil-based monitor system of the ElectronFlash machine (Fig. 11).

A decreasing trend of response as a function of the accumulated dose could be suspected, but the response after 200 kGy is still compatible with that of the virgin detector.

Fig. 4 PDD curves with 6-mm spherical UCD and flashDiamond at 7 MeV. The associated bars are only shown on UCD for a better inspection of the graphs

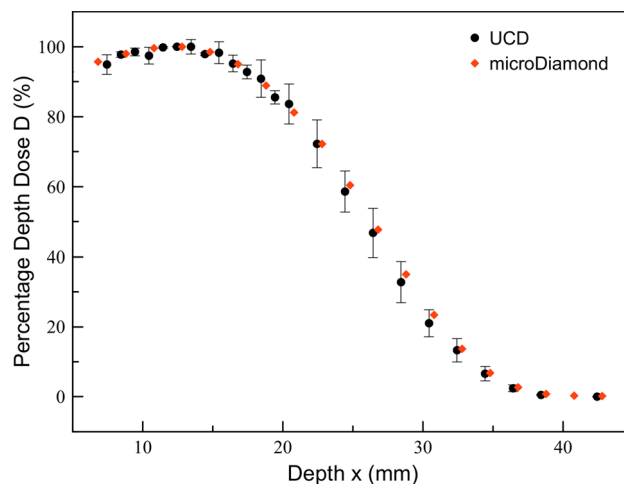


Fig. 5 PDD curves with 6-mm spherical UCD and flashDiamond at 9 MeV. The associated bars are only shown on UCD for a better inspection of the graphs

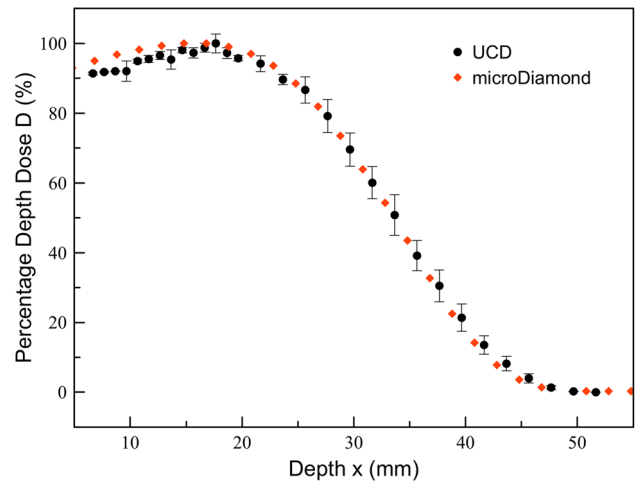


Fig. 6 Lateral beam profiles with UCD (6 mm diameter) and flashDiamond at 7 MeV. The associated bars are only shown on UCD for a better inspection of the graphs. Data are normalised to the value at $d = 0$

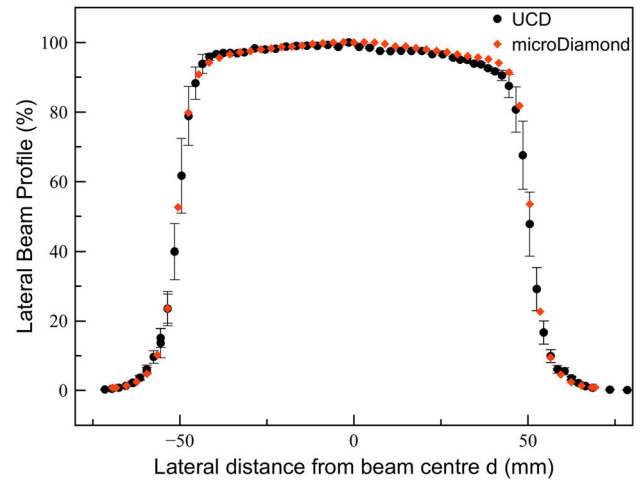


Fig. 7 Lateral beam profiles with UCD (6 mm diameter) and flashDiamond at 7 MeV. The associated bars are only shown on UCD for a better inspection of the graphs. Data are normalised to the value at $d = 0$

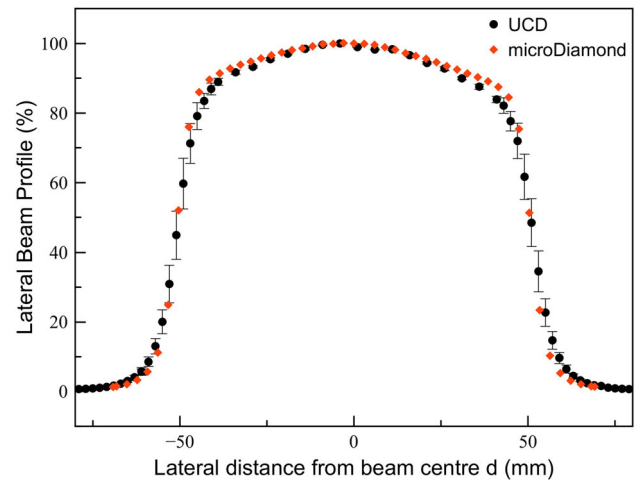


Fig. 8 UCD linearity in terms of dose per pulse

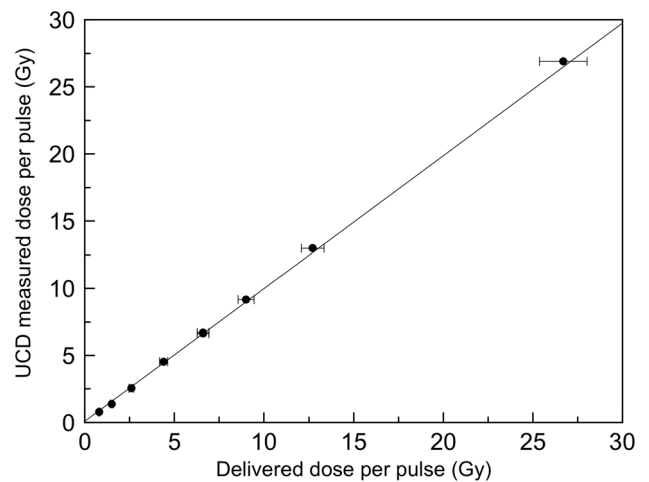


Fig. 9 Experimental setup for the study of UCD (6 mm diameter) angular response

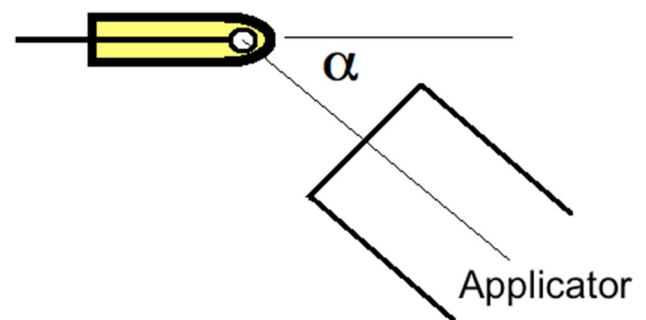
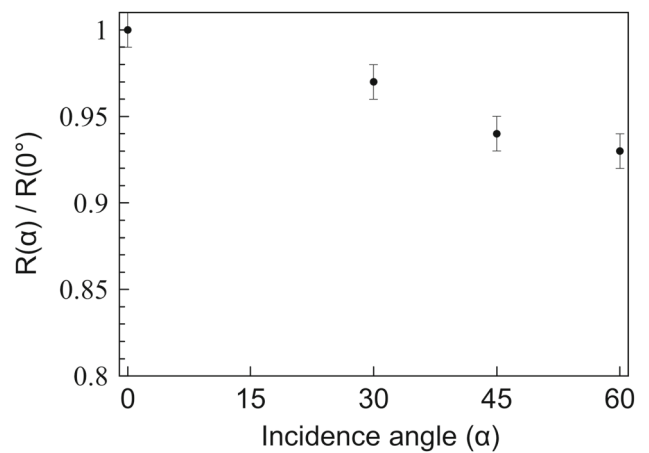


Fig. 10 UCD (6 mm diameter) angular response. Values are normalized to their maximum obtained at $\alpha = 0^\circ$

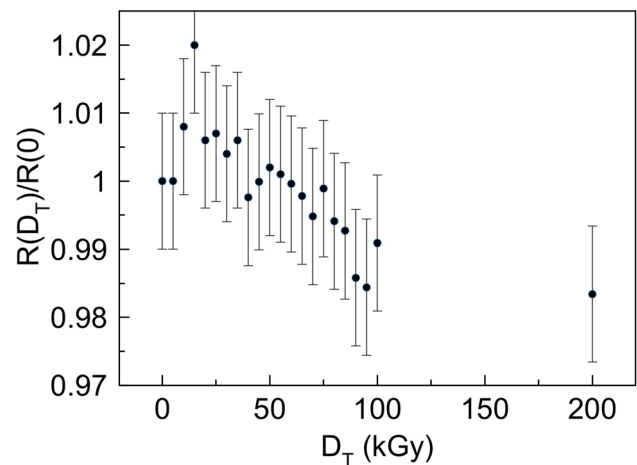


4 Conclusions

The Unbalanced Core Detector (UCD) was proposed as a novel type of electron dosimeter for FLASH Radiotherapy. This device was tested using 7 and 9 MeV flash electron beams from an ElectronFlash accelerator. The measured spatial dose distributions in water phantom are equivalent to those obtained with the existing flashDiamond dosimeter. In addition, the UCD demonstrated very high radiation resistance, linear operation up to 6 MGy s^{-1} , and the possibility to acquire the time evolution of a single radiation pulse. The angular response was preliminarily assessed in air, finding a response loss of 7% when the incidence angle varies from 0° to 60° . To thoroughly assess this characteristic, an experiment in water is planned for the near future.

Although more investigation is needed to extend the understanding of the energy dependence and to improve the temporal description of the pulses, UCD can be proposed as a convenient and highly qualified dosimeter in view of the clinical translation of FLASH Radiotherapy.

Fig. 11 Evolution of the UCD (6 mm diameter) response as a function of the accumulated dose at 9 MeV. In X-axis is reported the absorbed dose determined from the toroidal coil-based monitor system, after calibration against radiochromic films. In Y-axis is reported the UCD reading per unit absorbed dose normalized to the same value for the virgin detector



Acknowledgements The development of the Unbalanced Core Detector (UCD) was funded under the project INFN R4I 2022 FLASHDOS. The beam time was freely provided by SIT Sordina IORT Technologies S.P.A. under the research agreement TTB_21LNF_136.

Funding Open access funding provided by Ente per le Nuove Tecnologie, l'Energia e l'Ambiente within the CRUI-CARE Agreement.

Data Availability Statement Data sets generated during the current study are available from the corresponding author on reasonable request. The manuscript has associated data in a data repository.

Open Access This article is licensed under a Creative Commons Attribution 4.0 International License, which permits use, sharing, adaptation, distribution and reproduction in any medium or format, as long as you give appropriate credit to the original author(s) and the source, provide a link to the Creative Commons licence, and indicate if changes were made. The images or other third party material in this article are included in the article's Creative Commons licence, unless indicated otherwise in a credit line to the material. If material is not included in the article's Creative Commons licence and your intended use is not permitted by statutory regulation or exceeds the permitted use, you will need to obtain permission directly from the copyright holder. To view a copy of this licence, visit <http://creativecommons.org/licenses/by/4.0/>.

References

- H. Weiss et al., Oxygen depletion in cells irradiated at ultra-high dose-rates and at conventional dose-rates. *Int. J. Radiat. Biol. Relat. Stud. Phys. Chem. Med.* **26**, 17–29 (1974). <https://doi.org/10.1080/09553007414550901>
- H. Weiss et al., An equation for predicting the surviving fraction of cells irradiated with single pulses delivered at ultra-high dose rates. *Radiat. Res.* **50**, 441–452 (1972). <https://doi.org/10.2307/3573501>
- S. Hornsey et al., Unexpected dose-rate effect in the killing of mice by radiation. *Nature* **9**(210), 212–213 (1966). <https://doi.org/10.1038/210212a0>
- S.B. Field et al., Effects of dose-rate on the radiation response of rat skin. *Int. J. Radiat. Biol. Relat. Stud. Phys. Chem. Med.* **26**, 259–267 (1974). <https://doi.org/10.1080/09553007414551221>
- V. Favaudon et al., Ultrahigh dose-rate FLASH irradiation increases the differential response between normal and tumor tissue in mice. *Sci. Transl. Med.* (2014). <https://doi.org/10.1126/scitranslmed.3008973>
- J. Bourhis et al., Clinical translation of FLASH radiotherapy: Why and how? *Radiother. Oncol.* **139**, 11–17 (2019). <https://doi.org/10.1016/j.radonc.2019.04.008>
- B. Lin et al., FLASH radiotherapy: history and future. *Front. Oncol.* (2021). <https://doi.org/10.3389/fonc.2021.644400>
- M.C. Vozenin, J. Bourhis, M. Durante, Towards clinical translation of FLASH radiotherapy. *Nat. Rev. Clin. Oncol.* **19**(12), 791–803 (2022). <https://doi.org/10.1038/s41571-022-00697-z>
- J.D. Wilson et al., Ultra-high dose rate (FLASH) radiotherapy: Silver bullet or fool's gold? *Front. Oncol.* **9**, 1563 (2020). <https://doi.org/10.3389/fonc.2019.01563>
- N. Esplen, M.S. Mendonca, M. Bazalova-Carter, Physics and biology of ultrahigh dose-rate (FLASH) radiotherapy: a topical review. *Phys. Med. Biol.* **65**(23), 2303 (2020). <https://doi.org/10.1088/1361-6560/abaa28>
- M.C. Vozenin et al., The advantage of FLASH radiotherapy confirmed in mini-pig and cat-cancer patients. *Clin. Cancer Res.* **25**(1), 35–42 (2019). <https://doi.org/10.1158/1078-0432.CCR-17-3375>
- R. MacKay et al., FLASH radiotherapy: considerations for multibeam and hypofractionation dose delivery. *Radiother. Oncol.* **164**, 122–127 (2021). <https://doi.org/10.1016/j.radonc.2021.09.011>
- P. Montay-Gruel et al., Long-term neurocognitive benefits of FLASH radiotherapy driven by reduced reactive oxygen species. *Proc. Natl. Acad. Sci.* **116**(22), 10943–10951 (2019). <https://doi.org/10.1073/pnas.1901777116>
- J. Bourhis et al., Treatment of a first patient with FLASH-radiotherapy. *Radiother. Oncol.* **139**, 18–22 (2019). <https://doi.org/10.1016/j.radonc.2019.06.019>
- O. Gaide et al., Comparison of ultra-high versus conventional dose rate radiotherapy in a patient with cutaneous lymphoma. *Radiother. Oncol.* **174**, 87–91 (2022). <https://doi.org/10.1016/j.radonc.2021.12.045>
- P. Montay-Gruel et al., X-rays can trigger the FLASH effect: ultra-high dose-rate synchrotron light source prevents normal brain injury after whole brain irradiation in mice. *Radiother. Oncol.* **129**, 582–588 (2018). <https://doi.org/10.1016/j.radonc.2018.08.016>

17. A.R. Kennedy et al., Implementation, and in vivo validation of a novel proton FLASH radiation therapy system. *Radiat. Oncol. Biol. Phys.* **106**, 440–448 (2020). <https://doi.org/10.1016/j.ijrobp.2019.10.049>
18. W. Tinganelli et al., FLASH with carbon ions: tumor control, normal tissue sparing, and distal metastasis in a mouse osteosarcoma model. *Radiother. Oncol.* **175**, 185–190 (2022). <https://doi.org/10.1016/j.radonc.2022.05.003>
19. M.C. Vozenin et al., Biological benefits of ultra-high dose rate FLASH radiotherapy: sleeping beauty awoken. *Clin. Oncol. (R. Coll. Radiol.)* **31**(7), 407–415 (2019). <https://doi.org/10.1016/j.clon.2019.04.001>
20. D.R. Spitz et al., An integrated physico-chemical approach for explaining the differential impact of FLASH versus conventional dose rate irradiation on cancer and normal tissue responses. *Radiother. Oncol.* **139**, 23–27 (2019). <https://doi.org/10.1016/j.radonc.2019.03.028>
21. M. Jaccard et al., High dose-per-pulse electron beam dosimetry: Commissioning of the oriatron eRT6 prototype linear accelerator for preclinical use. *Med. Phys.* **45**, 863–874 (2018). <https://doi.org/10.1002/mp.12713>
22. R. Moeckli et al., Commissioning of an ultra-high dose rate pulsed electron beam medical LINAC for FLASH RT preclinical animal experiments and future clinical human protocols. *Med. Phys.* **48**, 6 (2021). <https://doi.org/10.1002/mp.14885>
23. F. Di Martino et al., FLASH radiotherapy with electrons: issues related to the production, monitoring, and dosimetric characterization of the beam. *Front. Phys.* (2020). <https://doi.org/10.3389/fphy.2020.570697>
24. L. Giuliano et al., Characterization of ultra-high-dose rate electron beams with electron flash LINAC. *Appl. Sci.* **13**, 631 (2023). <https://doi.org/10.3390/app13010631>
25. S. Siddique, H.E. Ruda, J.C.L. Chow, FLASH radiotherapy and the use of radiation dosimeters. *Cancers* **15**(15), 3883 (2023). <https://doi.org/10.3390/cancers15153883>
26. M. Gondré, P.G. Jorge, M.C. Vozenin, J. Bourhis, F. Bochud, C. Bailat, R. Moeckli, Optimization of alanine measurements for fast and accurate dosimetry in FLASH radiation therapy. *Radiat. Res.* **194**(6), 573–579 (2020). <https://doi.org/10.1667/RR15568.1>
27. F. Romano et al., Ultra-high dose rate dosimetry: challenges and opportunities for FLASH radiation therapy. *Med. Phys.* **49**, 4912–4932 (2022). <https://doi.org/10.1002/mp.15649>
28. F. Gómez et al., Development of an ultra-thin parallel plate ionization chamber for dosimetry in FLASH radiotherapy. *Med. Phys.* **49**, 4705–4714 (2022). <https://doi.org/10.1002/mp.15668>
29. F. Di Martino et al., A new solution for UHDP and UHDR (Flash) measurements: theory and conceptual design of ALLS chamber. *Phys. Med.* **102**, 9–18 (2022). <https://doi.org/10.1016/j.ejmp.2022.08.010>
30. M. Marinelli et al., Design, realization, and characterization of a novel diamond detector prototype for FLASH radiotherapy dosimetry. *Med. Phys.* **49**, 1902–1910 (2022). <https://doi.org/10.1002/mp.15473>
31. F. Romano et al., First characterization of novel silicon carbide detectors with ultra-high dose rate electron beams for FLASH radiotherapy. *Appl. Sci.* **13**, 2986 (2023). <https://doi.org/10.3390/app13052986>
32. M. Pimpinella et al., Energy dependence of PTW microdiamond detector in radiotherapy photon and electron beams. *Phys. Med.* **3**, e64 (2014). <https://doi.org/10.1016/j.ejmp.2014.07.195>